

Chapter 6

Utilizing Cone Penetration Tests for Landslide Evaluation

M.E. Jorat, S. Kreiter, T. Mörz, V. Moon, and W. de Lange

Abstract Pore pressure and shear strength are two important parameters that control the stability of slopes. These parameters can be derived *in-situ* by cone penetration testing (CPT) with pore pressure measurements. This paper presents the results from three static, vibratory and dissipation CPT profiles deployed into a landslide headwall at Pyes Pa, Bay of Plenty, New Zealand. The landslide strata consist of volcanic ashes and ignimbrites. Studying the stability of slopes in this area using *in-situ* geotechnical testing is of societal-economic importance since several other landslides within comparable strata caused considerable property damage. Three CPT profiles were collected across the headwall of the slide scar with 2 m spacing in undisturbed sediments using static, vibratory and dissipation test modes. Static CPT results are used to evaluate soil grain size variations, geotechnical parameters of sediments such as shear resistance, probable slip surface and sensitivity of sediments. Liquefaction potential of sediments is assessed using vibratory CPT results. For dissipation tests, the cone remained stationary in the sediment for ~60 min to monitor pore pressure dissipation at the depths of 6, 9 and 11 m. With the use of pore pressure dissipation data, values of soil horizontal permeability are calculated. The liquefaction probability from static CPT results is compared to liquefaction potential evaluation from vibratory CPT. Last but not least, an unstable soil layer is defined based on static CPT, vibratory CPT and dissipation results.

Keywords CPT • Landslide • Static • Vibratory • Dissipation

M.E. Jorat (✉) • S. Kreiter • T. Mörz
Marum – Center for Marine and Environmental Sciences, University of Bremen, Klagenfurter
Strasse, 28359 Bremen, Germany
e-mail: jorat@uni-bremen.de

V. Moon • W. de Lange
Department of Earth and Ocean Sciences, University of Waikato, Private Bag 3105, Hamilton
3240, New Zealand

6.1 Introduction

Slope failure is an important factor which causes damage to public and private properties every year. Slope failure can be manifested as landslides and may destroy or damage buildings and infrastructure located on or in the path of a landslide (Ozcep et al. 2010). In extensive areas of New Zealand, prevalent severe landslides result from intensive rainstorms or prolonged winter wetness (Trustrum et al. 1984). Infiltration of rainwater into soil increases the pore water pressure which reduces the effective stresses and alters structure of soil that finally results in a reduction or even elimination of frictional and cohesive strength (Reddi 2003). Protracted and intense rainfall in New Zealand dramatically increases pore water pressure in soils which boosts shear stresses on materials and causes slopes to fail (Brown 1983). Slope failures induced by excessive rainfall may cause shallow landslides which trigger small volumes of earth and/or debris with considerable velocity and high impact energy (Giannecchini et al. 2012).

There have been several studies on different landslides in New Zealand (e.g. Brown 1983). In this paper, a landslide which is located at Pyes Pa, Bay of Plenty, New Zealand is geotechnically investigated as a typical example of a shallow onshore landslide. We describe its morphological and structural characteristics and discuss the possible mechanism of emplacement by using static, vibratory and dissipation cone penetration data. With static CPT (SCPT) data, soil behavior type, undrained shear strength, sensitivity and liquefaction potential are calculated. Vibratory CPT (VCPT) is performed to evaluate liquefaction potential by a second measurement. Permeability properties of layers are evaluated with the use of CPT dissipation test.

In-situ cone penetration test measurements were undertaken at three different locations at 463 Pyes Pa Road, Tauranga, New Zealand (Fig. 6.1). Table 6.1 shows SCPT, VCPT and dissipation test locations which were performed at Pyes Pa landslide to evaluate the static, dynamic and permeability behavior of soil.

6.2 Site Characterization

The geology of the Tauranga area consists of Pliocene to Pleistocene volcanic materials derived predominantly from the Taupo Volcanic Zone; the materials are mainly rhyolitic in composition. At the study site, Late Pleistocene and Holocene tephras from the surface horizons overlie fluvial sands and silts and older pyroclastic units. Below these, the Waimakariri Ignimbrite, a partially welded pumice-rich ignimbrite, overlies the non-welded Te Ranga Ignimbrite (Briggs et al. 1996). Houghton et al. (1995) suggest that the Waimakariri Ignimbrite has an age between 0.32 and 0.22 Ma. Based on visual inspection at the landslide area, the first 3 m of the soil profile consists of an ash sequence that continues with a paleosol layer from 3 to 6.80 m. From the depth of 7–13.70 m, a clayey layer was observed, which

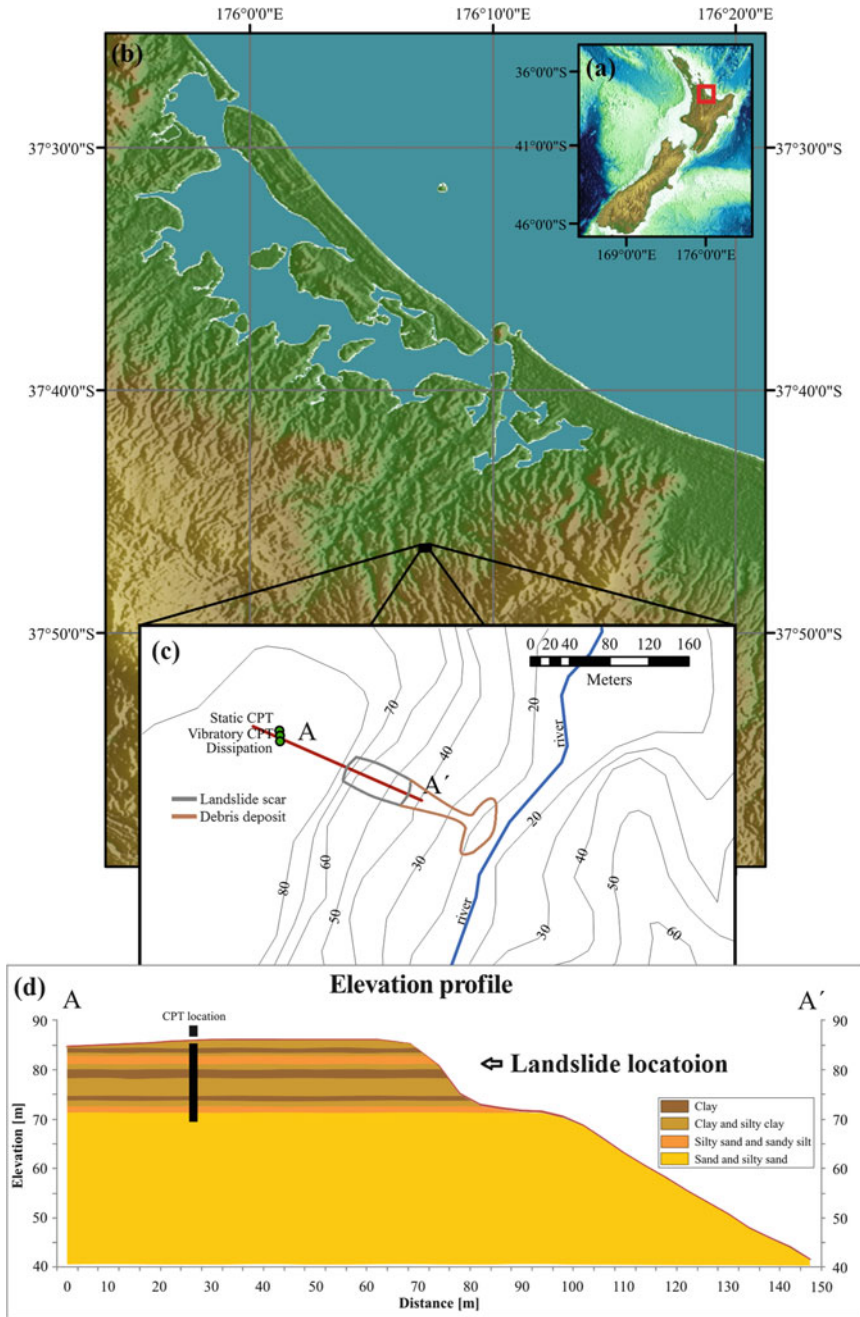


Fig. 6.1 Map of (a) New Zealand, (b) Bay of Plenty, (c) Topography, landslide location and location of CPTs at Pyes Pa and (d) landslide cross section. “Map a, b and c are generated from LINZ (Land Information New Zealand) data” Layering at (d) is derived from soil behavior type calculated by SCPT

Table 6.1 Cone penetration test location details in Pyes Pa landslide

CPT location/Type	Coordinate	
Static	37.774358° S	176.118563° E
Vibratory	37.774309° S	176.118561° E
Dissipation	37.774299° S	176.118527° E

likely contains halloysite with accumulation of clay at the base of the sequence. From the depth of 13.70–16 m, a poorly welded, loose and coarse grain sized ignimbrite was observed.

A river flows down the low lying valley floor that indicates the vicinity of the ground water table. According to Foundation Engineering Geotechnical and Environmental Consultant Company (2006), standing ground water levels were not encountered below the elevated and gently sloping portions of 52 Pyes Pa Road, suggesting free drainage of coarse volcanic particles. Yet, across the valley floor, they observed seepage of groundwater at a layer between 0.60 and 1 m. This indicates the presence of a complex ground water regime, with mostly free drainage due to the coarse nature of many of the primary pyroclastic units. However, perched water tables associated with local aquitards clearly exist. These aquitards are the result of the accumulation of secondary clay minerals, most commonly associated with weathering of fine-grained tephra units. The spatial distribution of these aquitards is difficult to predict.

6.3 Methods

6.3.1 *In-Situ CPT Measurements*

In-situ measurements of sediment physical and mechanical properties were carried out with a CPT unit which is called GOST. GOST, a new geotechnical offshore seabed CPT tool developed at University of Bremen, Center for Marine and Environmental Sciences (Marum), was utilized for the investigations (Fig. 6.2). GOST possesses a cone with a projected area of 5 cm². Compared with normal cones with projected area of 10 cm², 5 cm² cones react more sensitively and precisely to rapid changes in thin layered soils via the pore water pressure response, which leads to increased vertical resolution and provides more detailed profiles (Lunne et al. 1997; Hird and Springman 2006). The penetration rate for static tests is the standard rate of 2 cm/s (e.g. Lunne et al. 1997). The vibrocone used in this study was vertically forced with a frequency of 15 Hz and an amplitude of 25 mm.

SCPT, VCPT and dissipation tests were conducted within 1 m of each other. The tests were conducted in early autumn on 6th of March 2012. Rainfall in Tauranga is approximately evenly distributed throughout the year, with little seasonal variability. Instruments were transported to the location and positioned by truck crane, and a mobile generator was used to provide power for the instruments. Since GOST is designed and manufactured to work on/off shore, no modification was required to operate on land.



Fig. 6.2 Geotechnical Offshore Seabed Tool (GOST) sketch

Table 6.2 Classification of sensitive clays (Skempton and Northey 1952)

Sensitivity (S_t)	Classification
~1	Insensitive
1–2	Low sensitive
2–4	Medium sensitive
4–8	Sensitive
8–16	Extra sensitive
>16	Quick

6.3.2 Physical and Mechanical Properties

Soil behavior type (SBT) is evaluated based on SCPT results and the SBT chart through the CLiq (2008) software program based on the Robertson et al. (1986) classification scheme. Schmertmann (1978) explained that the sensitivity of soils is inversely related to the CPT friction ratio. He proposed a correlation for analyzing the sensitivity of sediments as follows:

$$S_t = N_s / R_f \quad (6.1)$$

Where, N_s is constant and R_f is friction ratio.

Lunne et al. (1997) suggested a value of $N_s = 7.5$ for mechanical CPT data. Skempton and Northey (1952) defined sensitivity of clay as a ratio of maximum undrained shear strength of undisturbed clay over maximum undrained shear strength of remolded clay. They proposed a classification for sensitive clay which is shown in Table 6.2.

Interpretation of undrained shear strength from CPT results was performed using total cone resistance (Lunne et al. 1997). In order to compare static and vibratory tip resistance, Sasaki et al. (1984) proposed a formula for direct comparison of these two values, which is defined as the reduction ratio (RR) and explained as:

$$RR = 1 - q_{cv} / q_{cs} \quad (6.2)$$

Where, RR is the reduction ratio, q_{cv} is the vibratory cone penetration resistance and q_{cs} is the static cone penetration resistance. Values of RR near unity demonstrate small measured values of q_{cv} compared with q_{cs} , an RR of zero identifies equal values of q_{cs} and q_{cv} (Bonita et al. 2004), while negative values of RR show greater q_{cv} than q_{cs} . The soil liquefaction potential index (LPI) is used to interpret the liquefaction susceptibility in terms of severity over depth which was developed based on methodology proposed by (Iwasaki 1986). He proposed four discrete categories based on the numeric value of LPI as follows:

LPI = 0	: Liquefaction risk is very low
0 < LPI <= 5	: Liquefaction risk is low
5 < LPI <= 15	: Liquefaction risk is high
LPI > 15	: Liquefaction risk is very high

GeoLogismiki, in collaboration with Gregg Drilling Inc. and Prof. Peter Robertson have developed a software which is called CLiq (2008). This program is a CPT based SBT and liquefaction assessment software. SBT is evaluated based on a chart proposed by Robertson et al. (1986) and soil liquefaction assessment procedure based on static CPT results is developed according to Robertson and Wride (1998). Robertson in 2009 revised his former procedure and that procedure is used in CLiq software for evaluation of liquefaction resistance of soils.

6.4 Results and Discussion

6.4.1 Static CPT

According to the origin of soil at the study area described in Sect. 6.2, ignimbritic layers showing different degrees of weathering interlayered with weathered ashes and other pyroclastites are the cause for changes in the CPT profile (Fig. 6.3). Specifying the location of saturated zones within the sequence is very important in interpreting the pore water pressure response during CPT. Pore water pressure values measured in unsaturated materials represent induced pore water pressures in response to the undrained loading applied by the cone penetration. In contrast, pore water pressure values measured within saturated zones represent these induced pressures, as well as the hydrostatic head associated with the standing water.

Below 13.7 m the measured pore water pressure rapidly falls, indicating that free-draining material lies below this level. This material is interpreted as ignimbrite

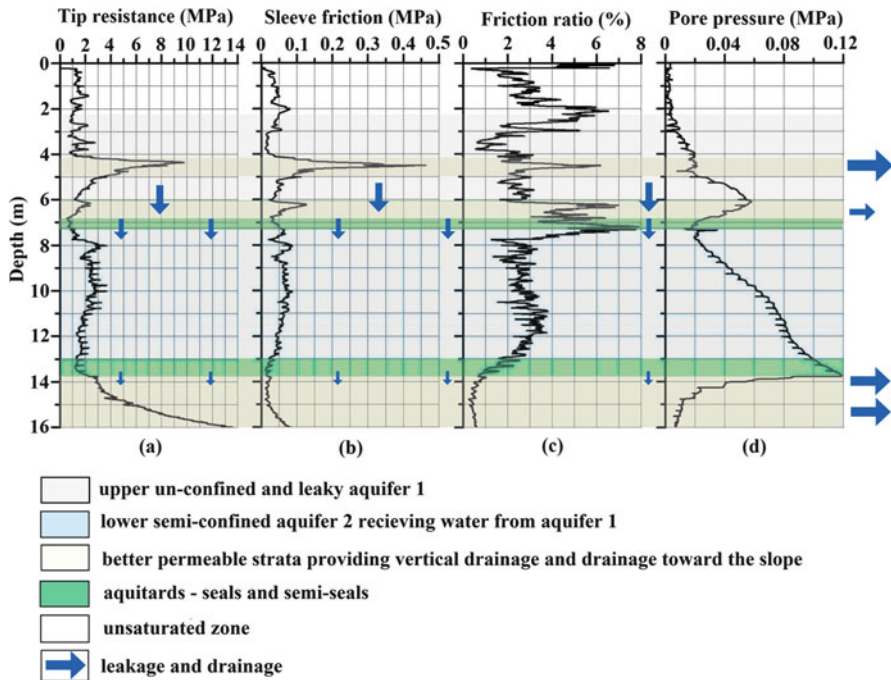


Fig. 6.3 Static CPT result (a) tip resistance, (b) sleeve friction, (c) friction ratio and (d) pore water pressure and hydrological situation of layers to a penetration depth of 16 m

based on the known local stratigraphy. This ignimbrite has a sandy, pumiceous texture with minimal weathering. The material is highly permeable and induced pore water pressures from the cone penetration are insignificant. Immediately above the ignimbrite, a rapid rise in pore water pressure with depth is seen from 12.5 to 13.7 m. This zone marks the transition from the lower, uniformly free-draining material to an overlying sequence of clay and silt materials that show marked variations in the pore water response. These layers are mostly tephra from different eruptive events and have variable textures associated with the characteristics of each eruption.

The primary textures are overprinted with different levels of weathering representing the time of exposure at the ground surface; this weathering is expressed in the clay content, and in the extreme can be seen as well-developed paleosols in the sequence. The hydrological conditions of these layers above 13.70 m are illustrated based on SCPT results (Fig. 6.3). A lower semi-confined aquifer 2 extends from 7.20 to 13 m, and is surrounded by two sealed and semi-sealed aquitards at 6.90–7.20 m and 13–13.70 m. Above this is an upper aquifer 1 which extends from the unsaturated zone to 6.90 m; this aquifer contains two better permeable strata. Aquifer 2 receives water from aquifer 1 through the semi-sealed overlying aquitard. The upper leaky and unconfined aquifer 1 and lower semi-confined aquifer 2 are responsible for the pore water pressure increase seen in the layer between 7.20

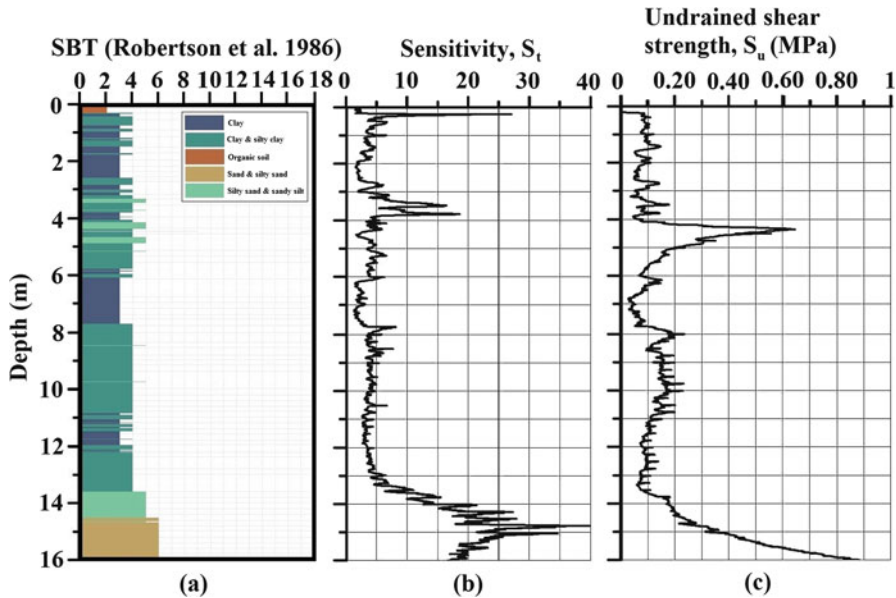


Fig. 6.4 CPT based (a) soil behavior type (b) sensitivity and (c) undrained shear strength calculated from SCPT results

and 13.70 m which is believed to represent both saturated pore pressure and an induced pore pressure signal due to penetration. The pore water pressure in the aquitard located at 6.90 to 7.20 m is low which is related to the permeable layer immediately above the aquitard that drains pore water from the upper unconfined and leaky aquifer and transfers it to lower semi confined aquifer 2. In contrast, because of the buildup of pore water pressure at the lower semi-confined aquifer 2 and very low permeability characteristics of the aquitard located at the depth of 13–13.70 m, pore water pressure is high at the depth of 13.70 m. This results in a reduction of effective stress. Therefore, excessive rainfall can result in the situation of zero effective stress at the depth of 13.70 m, leading to failure of the slope.

Taking the results of Fig. 6.4b and values of Table 6.2 into consideration, the first 14.60 m of soil layers are predominantly categorized as medium sensitive/sensitive materials. Two extra-sensitive layers occur within this sequence: from 3.20 to 3.80 m and from 13.70 to 14.60 m. The apparent rapid increase of sensitivity at the depth of 0.20 m resulted from great values of sleeve friction in organic soils (Figs. 6.3b and 6.4a). Given the coarse grain size of particles below the depth of 14.60 m, a sensitivity calculation cannot be applied for this layer. High sensitivity values of the layers between depths of 3.20–3.80 m and 13.70–14.60 m indicate a dramatic decrease of remolded undrained shear strength compared with undisturbed undrained shear strength. This indicates a vulnerability of the layers to disturbance. Accordingly, at circumstances like earthquakes, the respective layers would be potential slip surfaces.

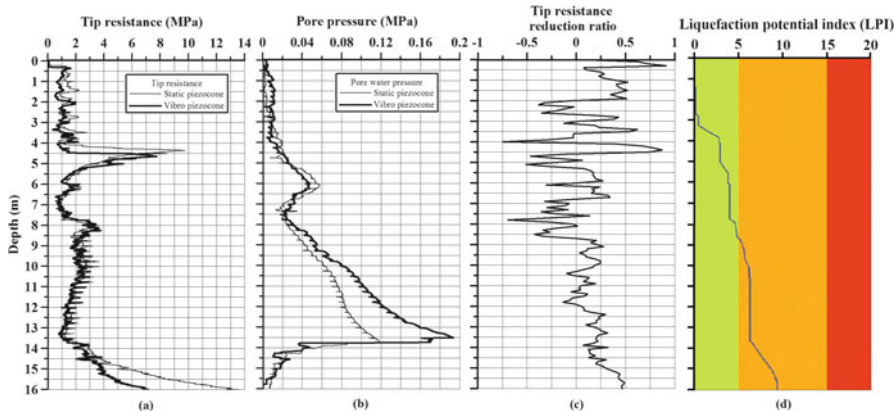


Fig. 6.5 Static and vibratory piezocone test results of (a) tip resistance and (b) pore water pressure (c) tip resistance reduction ratio. Calculated values of *RR*, *SCPT* and *VCPT* results are presented together to show the key role of vibration on sediments. (d) Soil liquefaction potential index analyzed by CLiq software using *SCPT* data

Undrained shear strength values are shown in Fig. 6.4c. From the depth of 8 m until 13.70 m, S_u decreased continuously. The same reduction trend is also observed in tip resistance, sleeve friction and friction ratio profiles of the same layer (Fig. 6.3a–c). On the other hand, pore water pressure at the respective layer increased progressively from the depth of 8 m and reached to its maximum at 13.70 m (Fig. 6.3d). Fine grained materials started from the depth of 8 m until 13.70 m, created a relatively impermeable layer which kept water during precipitation. Very low values of tip resistance, sleeve friction, friction ratio and undrained shear strength and an increased sensitivity at the depth of 13.70 m indicate the vulnerability of the layer to fail under the effect of driving forces. Accordingly, on the occasion of excessive rainfall, the weak soil layer located at the depth of 13.70 m would be considered as the most probable slip surface.

6.4.2 Vibratory CPT

A slight decrease in values of tip resistance under the effect of vibration is observed in the first 4 m of the *VCPT* profile (Fig. 6.5a), whilst the most significant reduction of tip resistance is observed at a layer between 4 m and 4.50 m. From 4.50 m until 13.70 m, static and vibratory tip resistances become compatible with each other and from 13.70 m until the end of *CPT* profile, vibratory tip resistance decreased progressively. Based on static and vibratory tip resistance, *RR* was defined (Fig. 6.5c). According to Tokimatsu (1988), soils with *RR* values more than about 0.80 have high liquefaction potential. Thus, the layer from 4 to 4.50 m is vulnerable to liquefaction. The 0.20 m of topsoil layer has $RR > 0.80$, however, since this layer consists of organic materials, it is not considered as a liquefiable layer (Fig. 6.4a).

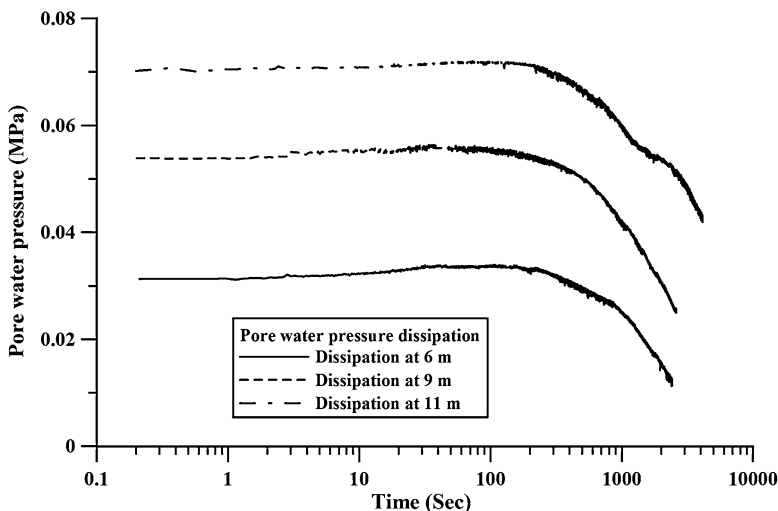


Fig. 6.6 Dissipation of pore water pressure vs. time performed at penetration depths of 6, 9 and 11 m following static cone penetration

An apparent increase of pore water pressure was observed under the effect of vibration at layer from 7.80 to 13.70 m (Fig. 6.5b). Konrad (1985) made an experiment to evaluate effects of cyclic loadings on saturated silty soils and based on his observations in all tested samples, the residual pore water pressure increased progressively with cycles of loading. Accordingly, a greater concentration of silt is verified at the above-mentioned layer which causes increased pore water pressure under the effect of vibration. With the increase of pore water pressure, effective stress decreases respectively. Maximum increase in pore water pressure under the effect of vibration occurred at the depth of 13.50 m which indicates the vulnerability of this layer to failure due to dynamic loads which are predominately induced by earthquake.

6.4.3 Dissipation Test

As can be observed from dissipation curves, pore water pressures first increased from an initial value to a maximum and then decreased to the hydrostatic value (Fig. 6.6). These kinds of dissipation curves are called non-standard dissipation curves (Chai et al. 2012). According to Teh and Houlsby (1991), volumetric expansion, resulting from movement of soil element from the tip to the sleeve of the penetrometer, is the possible reason for occurrence of non-standard dissipation curves.

According to Robertson (2010), the most precise soil permeability (k_h) estimation formula based on CPT dissipation tests is defined by the following equation:

$$k_h = (c_h \cdot \gamma_w) / M \quad (6.3)$$

Where: c_h is the coefficient of consolidation in the horizontal direction, γ_w is the unit weight of water and M is compressibility.

Robertson (2010) reported his findings to estimate 1-D constrained modulus (M) using:

$$M = \alpha_M (q_t - \sigma_{vo}) \quad (6.4)$$

When $I_c > 2.2$:

$$\alpha_M = Q_{tn} \text{ when } Q_{tn} \leq 14$$

$$\alpha_M = 14 \text{ when } Q_{tn} > 14$$

$$I_c = \left[(3.47 - \log Q_{tn})^2 + (\log F_r + 1.22)^2 \right]^{0.5} \quad (6.5)$$

$$F_r = [f_s / (q_t - \sigma_{vo})] \text{ 100\%} \quad (6.6)$$

$$Q_{tn} = [(q_t - \sigma_{vo}) / p_a] (p_a / \sigma'_{vo})^n \quad (6.7)$$

$$n = 0.381(I_c) + 0.05 (\sigma'_{vo} / p_a) - 0.15 \quad (6.8)$$

α_M = coefficient of constrained modulus

q_t = CPT corrected total cone resistance = $q_c + (1-a)u$

σ_{vo} = pre-insertion in-situ total vertical stress

p_a = reference atmospheric pressure = 100 kPa

I_c = soil behavior type index

Q_{tn} = normalized cone resistance

f_s = CPT sleeve friction

a = area ratio of the cone = (A_n/A_c)

σ'_{vo} = pre-insertion in-situ effective vertical stress

n = stress exponent

F_r = normalized friction ratio

To facilitate calculation of I_c , the value of the stress exponent (n) is assumed to be 1.

The most widely used formula for calculating c_h is the one proposed by Teh and Houlsby (1991):

$$c_h = (C_p \cdot r_0^2 \cdot I_r^{(0.5)}) / t_{50} \quad (6.9)$$

C_p = is a factor related to the location of the filter element and for a cone with shoulder filter element is equal to 0.245 (Teh and Houlsby 1991)

r_0 = radius of the cone

I_r = rigidity index

t_{50} = time required for 50 % of dissipation

$$I_r = G/s_u \quad (6.10)$$

$$G = \rho \cdot V_s^2 \quad (6.11)$$

Where, G is shear modulus, s_u is undrained shear strength, ρ is mass density (γ/g) and V_s is the shear wave velocity.

Hegazy and Mayne (1995) proposed a formula for shear wave velocity calculation based on CPT results which is as follows:

$$V_s = [10.10 \log q_t - 11.40]^{1.67} [f_s/q_t]^{0.30} \quad (6.12)$$

To calculate values of t_{50} , an equation which was proposed by Lunne et al. (1997) is introduced as follows:

$$U = (u_t - u_0)/(u_i - u_0) \quad (6.13)$$

Where, U is a degree of dissipation, u_t is pore pressure at time t , u_0 is *in-situ* equilibrium pore pressure and u_i is pore pressure at start of dissipation test.

Since the target is to calculate t_{50} for all dissipation tests, $U = 50\%$ is considered. According to the hydrological information of the study area as the ground water level was located down the slope and it was not touched by the cone during penetration, value of *in-situ* equilibrium pore pressure is considered to be zero. Having values of u_i from dissipation test, u_t at 50 % of dissipation is calculated. Accordingly, with the use of dissipation curves (Fig. 6.6), values of t_{50} are calculated.

Chai et al. (2012) proposed an empirical equation to correct the value of t_{50} for non-standard dissipation test as follows:

$$t_{50c} = t_{50} \left/ \left[1 + 18.50 \cdot (t_{u \max} / t_{50})^{0.67} \cdot (I_r/200)^{0.30} \right] \right. \quad (6.14)$$

Taking the above-mentioned equations into consideration, k_h in respective depths are calculated and presented in Table 6.3.

According to Table 6.3, values of k_h are very low in all samples which indicate the presence of fine grained materials in the layers. The lowest value of k_h is calculated at the depth of 9 m while the greatest value of k_h is achieved at the depth of 6 m.

The greatest value of k_h is achieved at the depth of 6 m which is located in the upper unconfined and leaky aquifer 1. As this point is situated above the permeable strata, it has greater permeability (Fig. 6.3). Values of k_h at depths of 9 and 11 m are very close to each other and are lower than k_h at the depth of 6 m. These points are located at the lower semi-confined aquifer 2 which is surrounded by aquitards at depths of 7 and 13.70 m.

Taking the very low horizontal permeability values of layers at depths of 9 and 11 m and pore water pressure condition of the layer between depths of 7.20–13.70 m into consideration the aquitard located at the depth of 13.70 m is considered as the most impermeable layer (Fig. 6.3). Because of this characteristic, at times of precipitation, infiltrated water cannot percolate rapidly toward the groundwater table causing excessive extra weight cumulating on the weakest and the most impermeable layers and increasing the failure potential of the slope.

6.4.4 Liquefaction Analysis with CLiq Software

Liquefaction potential index derived using SCPT data was analyzed by CLiq software and results are presented in Fig. 6.5d. Considering discrete categories of LPI proposed by Iwasaki (1986), the first 2.70 m of the profile has a very low risk for liquefaction (Fig. 6.5d). Soil layers between depths of 2.70 and 8.60 m are at low risk of liquefaction and from the depth of 8.60 m until the end of CPT profile, soil layers are potentially at high risk of liquefaction (Fig. 6.5d). The layer located at the depth of 13.70 m, which was indicated before as the most probable slip surface, is in the zone with high risk of liquefaction. Comparing the results of this section with the liquefaction probability evaluation discussed in the VCPT section, CLiq specifies greater areas with a risk of liquefaction than VCPT. Areas that CLiq indicates with high liquefaction potential by using SCPT data to make assumptions about cyclic behavior of layers are basically concentrated at the lower part of CPT profile while in VCPT, liquefiable layers are detected at the upper part of CPT profile by measuring the change in fabric upon small strain activation. For analysis of liquefaction in CLiq, the software considers coarse grain sized materials concentrated at the lower part of CPT profile as loose pulverized sand while these materials are actually the product of ignimbrite weathering and are not considered necessarily as pulverized sand which is the proof for a significant difference between the two methods.

Table 6.3 Horizontal soil permeability calculation details based on pore pressure dissipation test

Depth(m)	q_t (kPa)	V_s (m/s)	G (kPa)	I_r	t_{50} (sec)	$t_{u,max}$ (sec)	t_{50c} (sec)	C_{jt} (m ² /s)	F_r	Q_{in}	I_c	α_M	M (kPa)	k_h (m/s)
6	1,156.87	43.50	3,556.98	55.10	1,949	3,898	88	3.13E-06	2.21	8.48	2.98	8.48	8,359.97	3.67E-09
9	2,458.38	55.97	6,292.89	43.18	2,383	4,766	115	2.11E-06	2.04	10.19	2.90	10.19	22,429.16	9.23E-10
11	1,940.52	55.52	6,175.56	57.97	5,155	10,310	229	1.23E-06	2.76	6.72	3.21	6.72	10,905.37	1.11E-09

6.5 Summary and Conclusion

In this study a preliminary evaluation of the site conditions was made by using the map of the study area and site history as reported by published geological information. Static, vibratory and dissipation tests were performed by using the cone penetration test unit which is called GOST at the top of the slide scar. Cone penetration tests were performed to provide subsurface information. A static cone penetration test provided information in regard to soil grain size variations and the local strength variations with depth. The location of a possible slide plane was detected at a depth of 13.70 m based on low values of tip resistance, sleeve friction, undrained shear strength. Sensitivity of subsurface layers was also evaluated by using static cone penetration test results. The upper 14.60 m of layers were considered as medium sensitive/sensitive materials except for the layers between depths of 3.20 and 3.80 and 13.70 and 14.60 m which were identified as extra sensitive layers and indicated the vulnerability of the latter mentioned layers to disturbance. A vibratory cone penetration test was basically performed to evaluate subsurface layers liquefaction probability. Accordingly, the layer between depths of 4 and 4.50 m is potentially vulnerable to liquefaction. Pore water pressure increased under the effect of vibration in the layer between depths of 7.80 and 13.70 m which indicates the reduction of effective stresses under the effect of vibration. The maximum increase in pore water pressure happened at the depth of 13.70 m. Dissipation tests were performed at depths of 6, 9 and 11 m to evaluate the *in-situ* horizontal soil permeability at the respective depths. These measurements gave an average value of horizontal permeability of 1.9×10^{-9} m/s. The low values of horizontal permeability showed impermeable properties of layers above the proposed slip surface. Least permeable layers provided a barrier to infiltrated rain water which causes extra weight on the slope. The extra weight is an important factor in triggering the slide. The CLiq software was used to evaluate soil layers liquefaction potential. The software results showed the layers between 8.60 and 16 m to be at high risk for liquefaction. The software was unable to specify any liquefiable layer at the first 8.60 m of cone penetration test profile while vibratory cone penetration test specifies vulnerable layers to liquefaction in that area. Software considered coarse grain sized materials located at the bottom of the CPT profile as the pulverized sand and reported high risk of liquefaction for the respective layers while the materials are weathered ignimbrite.

In conclusion, based on static CPT, Vibratory CPT and dissipation test, the layer located at the depth of 13.70 m is identified as the most probable slip surface. The landslide is a shallow translational slide with a length of approximately 30 m and 6 m wide, and is formed on a slope of 27° . This equates to the scarp base at approximately 14 m depth. The lower portion of the scarp itself is covered by debris, but ignimbrite is exposed immediately below the base of the scarp. Therefore, the depth of 13.7 m observed in the CPT results is believed to be entirely consistent with the geomorphic evidence of the scarp face.

In this investigation cone penetration testing provided valuable information in landslide characterization when evaluated in conjunction with topographical and geological information.

Acknowledgment The authors acknowledge funding by Deutsche Forschungsgemeinschaft (DFG) via the Integrated Coastal Zone and Shelf Sea Research Training Group INTERCOAST and the MARUM Center for Marine Environmental Science at the University of Bremen. We would like to thank the Department of Earth and Ocean Sciences at University of Waikato for their help and support during the project, and Mr and Mrs Lucas for access to the site. We appreciate the effort of Prof. Dr. Hafliði Hafliðson from University of Bergen and Prof. Dr. Kate Moran from University of Victoria for reviewing the manuscript. Special thanks to Mr. Wolfgang Schunn for managing instruments and operation CPT unit.

References

- Bonita J, Mitchell JK, Brandon TL (2004) The effect of vibration on the penetration resistance and pore water pressure in sands. In: da Fonseca V, Mayne PW (eds) Proceedings of the ISC-2 on geotechnical and geophysical site characterization. Millpress, Rotterdam, pp 843–851
- Briggs RM, Hall GJ, Harmsworth GR, Hollis AG, Houghton BF, Hughes GR, Morgan MD, Whitbread-Edwards AR (1996) Geology of the Tauranga area. Sheet U14 1:50,000. Occasional report 22. Department of Earth Sciences, University of Waikato, Hamilton, New Zealand
- Brown WJ (1983) The changing imprint of the landslide on rural landscapes on New Zealand. *Landscape Plan* 10:173–204
- Chai J, Sheng D, Carter JP, Zhu H (2012) Coefficient of consolidation from non-standard piezocone dissipation curves. *Comput Geotech* 41:13–22
- CLiQ (2008) Geologismiki. Geotechnical liquefaction software at <http://www.geologismiki.gr/>
- Foundation Engineering Geotechnical and Environmental Consultants (2006) Geotechnical investigation report on proposes rural residential subdivision at 52 Pyes Pa Road, Tauranga, For Pyes Pa Investments Limited. Project No. 12921, pp 77–99
- Giannecchini R, Galanti Y, D' Amato Avanzi G (2012) Critical rainfall thresholds for triggering shallow landslides in the Serchio River Valley (Tuscany, Italy). *Nat Hazard Earth Syst Sci* 12:829–842
- Hegazy YA, Mayne PW (1995) Statistical correlations between V_s and cone penetration data for different soil types. In: Proceedings of the international symposium on cone penetration testing. CPT'95, vol 2. Swedish Geotechnical Society, Linköping, Sweden, pp 173–178
- Hird CC, Springman SM (2006) Comparative performance of 5 cm² and 10 cm² piezocones in a lacustrine clay. *Geotechnique* 56(6):427–438
- Houghton BF, Wilson CJN, McWilliams MO, Lanphere MA, Weaver SD, Briggs RM, Pringle MS (1995) Chronology and dynamics of a large silicic magmatic system: central Taupo Volcanic Zone, New Zealand. *Geology* 23:13–16
- Iwasaki T (1986) Soil liquefaction studies in Japan: state-of-the-art. *Soil Dyn Earthq Eng* 5(1):2–70
- Konrad J-M (1985) Undrained cyclic behaviour of Beaufort sea silt. In: Proceedings of Arctic'85, ASCE, San Francisco, 25–27 March, pp 830–837
- Lunne T, Robertson PK, Powell JJM (1997) Cone penetration testing in geotechnical practice. Taylor & Francis Group, London and New York
- Ozcep F, Erol E, Saracoglu F, Haliloglu M (2010) Seismic slope stability analysis: Gurpinar (Istanbul) as a case history. *Sci Res Essays* 5(13):1615–1631
- Reddi LN (2003) Seepage in soils. Wiley, Hoboken, p 07030

- Robertson PK (2009) Performance based earthquake design using the CPT. Keynote lecture, In: International conference on performance-based design in earthquake geotechnical engineering – from case history to practice, IS Tokyo, June 2009
- Robertson PK (2010) Estimating in-situ soil permeability from CPT & CPTu. In: 2nd international symposium on cone penetration testing, Huntington Beach, CA, USA. vol 2–3, Technical Papers, session 2, Interpretation, paper No. 51
- Robertson PK, Wride CE (1998) Evaluating cyclic liquefaction potential using the cone penetration test. *Can Geotech J* 35:442–459
- Robertson PK, Campanella RG, Gillespie D, Greig J (1986) Use of Piezometer cone data. In: In-situ '86 use of in-situ testing in geotechnical engineering. GSP 6, ASCE, Reston, VA, Specialty Publication, pp 1263–1280
- Sasaki Y, Itoh Y, Shimazu T (1984) A study on the relationship between the results of vibratory cone penetration tests and earthquake-induced settlement of embankments. In: Proceedings, 19th annual meeting of JSSMFE, Tokyo, Japan
- Schmertmann JH (1978) Guidelines for cone penetration test, performance and design. US Federal Highway Administration, Washington, DC, Report, FHWA-TS-78-209, p 145
- Skempton AW, Northey RH (1952) The sensitivity of clay. *Geotechnique* 3(1):30–53
- Teh CI, Housby GT (1991) An analytical study of the cone penetration test in clay. *Geotechnique* 41(1):17–34
- Tokimatsu K (1988) Penetration tests for dynamic problems. Penetration testing 1988, vol 1, In: Proceedings of the ISOPT-1, Balkema, Rotterdam, pp 117–136
- Trustrum NA, Thomas VG, Lambert MG (1984) Soil slip erosion as a constraint to hill country pasture production. *Proc NZ Grassl Assoc* 45:66–71